PAPER • OPEN ACCESS

Quasi-steady radiation of sound from turbulent sonic ergoregions

New Journal of Physics
The open access journal at the forefront of physics

Deutsche Physikalische Gesellschaft DPG
IOP Institute of Physics

Published in partnership with: Deutsche Physikalische Gesellschaft and the Institute of Physics

OPEN ACCESS

RECEIVED
27 February 2018

REVISED
1 August 2018

ACCEPTED FOR PUBLICATION
3 August 2018

PUBLISHED
14 August 2018

PAPER

Quasi-steady radiation of sound from turbulent sonic ergoregions

R Bürkle, A Gaidoukov and J R Anglin

Fachbereich Physik and State Research Center OPTIMAS, Technische Universität Kaiserslautern, D-67663 Kaiserslautern, Germany

E-mail: rbuerkle@physik.uni-kl.de

Keywords: sonic black holes, analog gravity, dynamical instabilities, superfluid turbulence, pre-thermalization

Abstract

Sonic Hawking radiation has recently been observed in dilute Bose–Einstein condensates (BECs), but it remains an open question whether this landmark achievement of atomic physics can lead to new insights into the effects on Hawking radiation of nonlinear back-reaction and new short-distance physics, as was originally hoped by Unruh when he introduced the sonic analogy. Furthermore, studies of sonic analog black holes have until now concentrated on (1+1)-dimensional scenarios, but Unruh's sonic analogy for curved spacetime is only valid in more than one spatial dimension. We therefore model the evolution of a (2+1)-dimensional sonic black hole in a dilute BEC, over a long enough time to let the initial Corley–Jacobson instabilities saturate in vortex production and give way to a long-lived quasi-stationary state. In this quasi-equilibrium state we find the initial laminar ergoregion replaced by a turbulent zone that steadily radiates sound, but with a non-thermal power spectrum.

1. Introduction

A black hole is among the simplest steady states in pure general relativity. Hawking's seminal 1974 paper [1] showed, however, that adding quantum fluctuations changes the black hole steady state into a thermally radiating one. The further addition of nonlinear back-reaction[1] is expected to make this state only quasi-steady, as the radiating black hole shrinks. Hawking's revised picture of the black hole steady state has suggested a deep connection between gravity, quantum mechanics, and thermodynamics, but the result is uncertain because new physics at trans-Planckian frequencies as well as quantum gravitational nonlinear back-reaction might revise the conclusion. On the other hand, string-theoretic models which embed general relativity as a classical limit within a nonlinear quantum theory have been shown to preserve black hole thermodynamics even while radically revising a black hole's basic nature [2].

It was with the explicit goal of gaining experimental insight into the sensitivity of black hole physics to short-distance and nonlinear corrections that Unruh proposed studying sonic horizons in fluids [3][2]. The *ergoregion* inside a black hole corresponds, in this analogy, to a zone of locally supersonic fluid flow; the surface at which the flow passes through the local speed of sound is the sonic horizon. There was and is no expectation that the nonlinear dynamics of any fluid would remain an exact analogy for full quantum gravity, but the original point of Unruh's analogy was simply to examine at least one example of a well-defined nonlinear quantum theory of

[1] By this term we mean all effects resulting from the full nonlinear theory that act back on the black hole and that are neglected in Hawking's derivation. In the context of analog gravity in BEC mean-field theory the full theory is the nonlinear Gross–Pitaevskii theory; neglecting the nonlinear back-reaction corresponds to the linear Bogoliubov approximation.

[2] From [3] above: 'This system forms an excellent theoretical laboratory where many of the unknown effects that quantum gravity could exert on black hole evaporation can be modeled. ... At distances of 10^{-8} cm, the assumptions ... of a smooth background flow are no longer valid just as in gravity one expects the concept of a smooth space–time on which the various relativistic fields propagate to break down at scales of 10^{-33} cm. Furthermore, the phonons emitted are quantum fluctuations of the fluid flow and thus affect their own propagation in exactly the same way that graviton emission affects the space–time on which the various relativistic fields propagate.' In the last sentence Unruh cannot really have meant that quantum gravity must be exactly like hydrodynamics, but rather just that nonlinear back-reaction of some kind will surely occur in both quantum gravity and hydrodynamics—and that this is a reason for pursuing analog experiments.

which the linearized long-wavelength limit corresponds to massless quantum fields in curved background spacetime.

The physics of sonic horizons has since grown into a topic in its own right [4–8]. The hypothesis that the full Hawking scenario of steady thermal radiation in horizon scenarios in general might be insensitive to short-distance details has been disproven by the discovery that finite ergoregions in fluids with supersonic dispersion at short wavelengths are dynamically unstable ('black hole lasing') [9–12]. Other theoretical studies have also shown that many dynamically linear aspects of the Hawking scenario can be investigated with BEC analogs, including quantum entanglement across the horizon due to parametric production of paired excitations [13–16]. Finally, analog Hawking radiation has actually been observed [17–19] in a quasi-one-dimensional Bose–Einstein condensate (BEC).

The time has come to revisit the original hopes for sonic black holes by examining nonlinear back-reaction in the analog system, even though it will not reproduce nonlinear quantum gravity, and even if it leads to steady states which are more like string-theoretic fuzzballs [2] than they are like general relativistic black holes. Long-term nonlinear evolution of a one-dimensional sonic horizon sustained by external pumping has been studied in [20], building on [21]. The system was found to evolve into a quasi-stationary phase of continuous emission of solitons (CESs) from the initial ergoregion, as also seen earlier in figure 5 of [10]. From the point of view of adding nonlinear dynamics to an analog spacetime, however, previous studies have been fundamentally limited by their concentration on one-dimensional scenarios (which are (1+1)-dimensional if time is included).

While actual experimental systems are of course three-dimensional, sufficiently tight spatial confinement of a quantum gas sample can restrict its hydrodynamic collective modes to a lower-dimensional subset of degrees of freedom, and the Unruh analogy with spacetime concerns only these hydrodynamic modes. The mapping [3] between the wave equations for sound in flowing fluid and for massless fields in curved spacetime with metric $g_{\mu\nu}$ is given in D spatial dimensions by

$$\begin{pmatrix} g_{00} & g_{0i} \\ g_{i0} & g_{ij} \end{pmatrix} = \left(\frac{\rho}{c}\right)^{\frac{2}{D-1}} \begin{pmatrix} |v|^2 - c^2 & -v_i \\ -v_i & \delta_{ij} \end{pmatrix}, \tag{1}$$

where ρ is the density, v the flow velocity and c the speed of sound of the fluid. The singularity of the prefactor for $D = 1$ reflects the fact that the mapping does not work for $D = 1$ (see our appendix for details). This means that no effectively (1+1)-dimensional fluid can be identified with any black hole metric.

One-dimensional systems can still serve as toy models whose long-wavelength sectors do possess causal (though not strictly metrical) horizons (see our appendix), but the full spacetime analogy requires at least two spatial dimensions. As far as strictly linear dynamics are concerned, one may also regard a (1+1)-dimensional model as the $k_\perp = 0$ or s-wave sector of a higher-dimensional system in which the background happens to have translational or rotational symmetry in the transverse directions [22]. Nonlinear dynamics will in general couple different transverse modes of the field together, however. For finite ergoregions, moreover, black hole-lasing instabilities will in general exist in many transverse modes, and so any translational or rotational symmetry in transverse directions will be unstable. Classically one could consider stationary states in which the unstable modes do not happen to be excited, but as soon as quantum fluctuations are taken into account, instabilities must grow. (See the appendix of [10] for a formal proof of this statement.)

In this paper we therefore show what happens as dynamical instabilities seeded by quantum vacuum noise grow from an initial horizon configuration in a spatially two-dimensional BEC. Using a single trajectory variant of the Truncated Wigner method [23–25], we incorporate nonlinear back-reaction at the classical level (i.e., in Gross–Pitaevskii mean-field theory) while modeling quantum fluctuations with Gaussian noise in the initial state. We find that linear dynamical instability of the initial laminar flow, as identified within Bogoliubov–de Gennes (BdG) perturbation theory for BEC backgrounds with finite ergoregions [10, 11], leads in two spatial dimensions to the proliferation of quantized vortices. This confirms that turbulent instabilities of trans-sonic flow, as anticipated by Unruh [3], persist in ultracold gases. Vortex production is also the expected generalization to higher dimensions of the soliton production seen in long-term evolution of quasi-one-dimensional sonic horizon models [20, 21]. After a transient epoch, our system relaxes to subsonic flow through a long quasi-stationary phase in which vortices and sonic noise are steadily emitted from the turbulent ergoregion, in qualitative resemblance to the fuzzball scenario [2]. We then analyze this quasi-steady regime in more detail.

2. Initial black-white-hole scenario

Following [10, 11], we consider a sonic horizon in a dilute BEC at zero temperature. In particular we study an idealized scenario in which the initial state of the BEC complex order parameter $\Psi(\boldsymbol{r}, t)$ is a small perturbation around a background Ψ_0 with uniform density ρ_0 and velocity v in the x-direction. We express all dimensionful

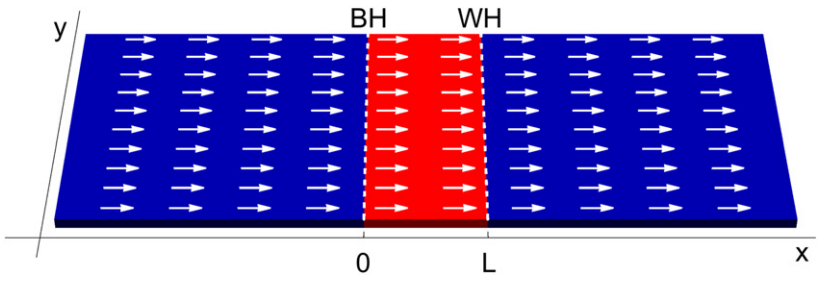

Figure 1. Initial set-up: two-dimensional BEC flowing with constant velocity in the x-direction. The local speed of sound is tuned in a steplike manner to create a small supersonic (red) region within subsonic flow (blue), making a black hole horizon at $x = 0$ and a white-hole horizon at $x = L$.

quantities in units defined by v, so that $t = \hbar\tau/(mv^2)$ and $\mathbf{r} = (x, y)\hbar/(mv)$, where m is the atomic mass. In these units we write $\Psi_0 = \sqrt{\rho_0}\exp(\mathrm{i}\boldsymbol{\nu}\boldsymbol{x})\exp(-\mathrm{i}\mu\tau)$ where $\boldsymbol{\nu} = (1, 0)$, and μ and ρ_0 are constants. Since experimental technology allows the tuning of inter-atomic interactions, the strength of the repulsive contact interaction $g > 0$ between the gas particles is assumed to be x-dependent, and an external potential $V(x)$ is tuned to compensate for it so that $\mu = 1/2v^2 + V(x) + g(x)\rho_0$ remains x-independent. The initial background Ψ_0 is then a stationary solution to the Gross–Pitaevskii equation (GPE)

$$\mathrm{i}\frac{\partial\Psi}{\partial\tau} = -\frac{1}{2}\boldsymbol{\nabla}^2\Psi + V(x)\Psi + g(x)|\Psi|^2\Psi \tag{2}$$

which defines the mean-field approximation [26].

Ψ_0 represents a sonic black hole/white-hole pair because within the ergoregion $0 < x < L$ the lower interaction strength $g(x)$ makes the local speed of sound $c(x) = \sqrt{g(x)\rho_0}$ lower than the initial background flow velocity v. See figure 1. This realization of a sonic ergoregion with constant Ψ_0 and non-uniform $g(x)$ is probably not the easiest experimental target, but it defines a simple initial state for quantum fluctuations: the condensate is prepared in the comoving-frame ground state with uniform $g(x)$, which is then suddenly altered to create the ergoregion.

The finite-size of our ergoregion, within a much larger subsonic region, is an important feature of our model because, as we will explain below, it implies dynamical instability. The fact that our system includes a white-hole as well as a black hole horizon is in contrast *not* of qualitative importance. Detailed study of sonic black holes sustained by atom sinks must await future work, but we have confirmed that two-dimensional all-black hole configurations with inward flow towards a 'singularity' represented by a localized imaginary potential behave very similarly to the simple black-white model. In effect our white horizon plays the role of the central sink in a finite black hole, without requiring us to model the outcoupling of atoms from a condensate.

As a further idealization, intended to represent a portion of a large horizon, we impose periodic boundary conditions in the y-direction; the width of our system is large enough that we detect no finite-size effects. In the x-direction our system is also periodic but with a length so great that no excitations propagate around it within the duration of our simulation. Since this duration is long enough to see complete relaxation of the initial black hole, the length in x of our system is large enough to be a computational challenge.

Our final idealization is to make the x-dependence of g and V be steplike, so that g takes a constant smaller value inside the ergoregion and a constant larger value outside it, leading to spatial abruptness of the transitions between sub- and supersonic flow. At least in one-dimension, however, it is easy to confirm by numerically solving the GPE that the qualitative behavior of BEC sonic horizons is insensitive to the details of the horizon profile. In a smoother background, behavior like that at our abrupt steps in g and V appears instead at semiclassical turning points[3]. The final parameters of our set-up are: the system lengths in x and y are $L_x = 2560\pi$ and $L_y = 40\pi$, respectively, while the ergoregion length is $L = 30$, all in our dimensionless units where the initial speed v is one. Our discrete spatial grid has spacing $d = 5\pi/64 \doteq 0.25$. We tune g and ρ_0 to make the speed of sound outside the ergoregion (and everywhere initially) be $c_1 = 1.5$, while inside the ergoregion (after it is turned on) it is $c_2 = 0.75$. The initial healing length is therefore $\xi = 1/c_1 = 2/3$ and our grid offers (somewhat) sub-healing-length resolution, while both L_y, $L \gg \xi$. GPE evolution is sensitive only to the combined product $g|\Psi|^2$; the initial values of g and ρ_0 separately are determined from considerations of quantum fluctuations.

[3] The results for a smooth but steep horizon profile in two-dimensions are very similar to the results presented here and will be published elsewhere [27].

3. Dynamical instabilities and nonlinearity

The linear stability of a stationary GPE solution like Ψ_0 is determined by evolving perturbations $\Psi = \Psi_0 + \delta\Psi$ under (2), while discarding terms of higher than linear order in $\delta\Psi$. The thus linearized GPE couples $\delta\Psi$ and $\delta\Psi^*$ in a system known as the BdG equations. The long-wavelength limit of BdG describes sound waves in a hydrodynamic background and can thus be mapped onto the field equation of a massless field in curved spacetime [3, 28], provided that $D > 1$ (see the appendix). At short wavelengths, however, BdG allows propagation faster than the speed of long-wavelength sound. This short-wavelength dispersion also implies, moreover, that the eikonal approximation must break down near a sonic horizon, requiring connection formulas which mix short- and long-wavelength modes [9, 11, 29]; such mixing also occurs at abrupt horizons like ours [11].

Analyzing this mixing at a single horizon reveals the remarkable result that, when the perturbations are quantized, the mixing with short-distance modes is not only compatible with long-wavelength Hawking radiation, but is actually the very mechanism by which Hawking radiation can occur in the black hole analog [9], because the connection formula resulting from continuity across the sonic horizon mixes BdG modes of opposite norm [29]. This mixing of negative and positive norms in the connection formula necessarily implies over-unity reflection at the horizon, however, for wave packets coming from inside the ergoregion. (Short-wavelength modes can propagate against the supersonic flow, and the fact that they are coupled to long-wavelength modes outside the ergoregion is an example of the kind of qualitative effect from short-distance physics that sonic black holes were intended to explore.) If the ergoregion is spatially finite, then reflected packets will encounter the horizon again and again after traversing the ergoregion, and repetitive over-unity reflection is exponential growth (see the discussion around figure 2 and 3 in [9]).

Thus the very mode-mixing which can generate analog Hawking radiation at a sonic horizon is also the mechanism of the 'black hole lasing' dynamical instability [9, 11, 12] of finite sonic black holes. Although this instability has received most study in ergoregions that are finite because they are 'sandwiched' between a black hole and a white-hole horizon as in our present model [9, 10, 12], section IV of [10] is devoted to a case of inward flow towards a sink, with no white-hole, and it shows that the instabilities persist (unless the ergoregion is too small for the spacetime analogy to be valid anyway). Over-unity reflection at the horizon for modes coming from inside the ergoregion is a destabilizing feature of any finite ergoregion; black hole lasing is not a pathology of white-hole horizons. The dynamical stability of a single planar black hole horizon with supersonic flow extending to infinity on one side simply represents the limit in which the ergoregion's crossing time, and therefore the instability growth time, have gone to infinity.

Since quantum fluctuations must always be present, growing modes can never just have zero amplitude (see the appendix of [10]). This means that the instabilities must grow until they are limited by nonlinearity and the BdG description breaks down. Linearized quantum field theory cannot describe this regime, but it can be described at the classical level by the GPE (2). This nonlinear classical theory also describes the evolution of the quantum gas well, if the *dilute gas parameter* α, which equals g for $D = 2$, is sufficiently small [30]. The derivation of the GPE as a saddlepoint approximation to the quantum field path integral is analogous to the derivation of Maxwell's equations from quantum electrodynamics to leading order in the fine structure constant: to leading order in α the quantum evolution in the Wigner representation is Liouvillian flow under the classical equations of motion. In the limit of small α, moreover, the Wigner functional of any stable quantum ground state approaches a narrow Gaussian ensemble.

Since $\alpha \lesssim 10^{-2}$ is common in quantum gas experiments ($\alpha = \sqrt{g^3\rho_0}$ in $D = 3$ [30], $\alpha = g$ in $D = 2$), one can use the GPE with appropriately noisy initial states to investigate what actually happens to sonic black holes. For large systems like ours evolving over long times, averaging over many runs is still time consuming. Since there are many degrees of freedom, however, each of which is an independent random variable, we propose that a single run from pseudo-random initial conditions chosen from the appropriate Gaussian ensemble will indicate the typical behavior of the whole ensemble [25]. This is the single trajectory variant of the Truncated Wigner method we use for our simulation.

Specifically, we evolve Ψ classically under (2), but from an initial condition $\Psi(x, y, 0) = \sqrt{\rho_0 + \delta\rho}\ \exp[\mathrm{i}(\theta_0 + \delta\theta)]$ with $\delta\rho, \delta\theta$ representing quantum fluctuations. These perturbations are random with a probability distribution given by the ground state Wigner function of the BdG excitations in a $\Psi_0 = \sqrt{\rho_0}\ \exp(\mathrm{i}\theta_0) = \sqrt{\rho_0}\ \exp(\mathrm{i}vx)$ background with completely uniform g and V equal to the values outside the ergoregion. This represents an experiment in which a uniform condensate is prepared at zero temperature, and then g and V within $0 < x < L$ are suddenly altered to create the ergoregion.

Since this Gaussian initial state includes fluctuations whose classical energy in each mode below the resolution cut-off would average $\hbar\omega/2$, it provides [28]

$$\langle \delta\rho^2(\boldsymbol{x})\rangle = \frac{\rho_0}{L_x L_y}\sum_{\boldsymbol{k}} \frac{|\boldsymbol{k}|\xi}{\sqrt{4 + |\boldsymbol{k}|^2\xi^2}} \doteq \frac{\rho_0}{d^2}, \tag{3}$$

$$\langle \delta\theta^2(\boldsymbol{x})\rangle = \frac{1}{\rho_0 L_x L_y}\sum_{\boldsymbol{k}} \frac{\sqrt{4+|\boldsymbol{k}|^2\xi^2}}{|\boldsymbol{k}|\xi} \doteq \frac{1}{\rho_0 d^2}, \tag{4}$$

where the sum is over $\boldsymbol{k}$ up to the cut-offs represented by the grid spacing d. Since the quantum initial state is not stationary under the classical evolution described by the GPE, but thermalizes to a classical distribution with a different temperature [23], we can only keep the truncated Wigner calculation accurate over our long simulation times by choosing ρ_0 large enough to keep $\sqrt{\langle\delta\rho^2\rangle}/\rho_0 \doteq (\rho_0 d^2)^{-1/2}$ small. As a conservative specific standard for 'small' we chose 10^{-2}, and to maintain this we took $\rho_0 = 4\times 10^4/d^2$. Since our simulation is two-dimensional, the initial sound speed $c_1 = 1.5$ implies the initially uniform $\alpha = g = c_1^2/\rho_0 = (15\pi/25600)^2 \doteq 3.4\times 10^{-6}$. If we interpret our two-dimensional model as representing a three-dimensional gas held within a vertical thickness of less than a healing length, this corresponds to an even smaller three-dimensional α, substantially lower than in experiments. The quantum and nonlinear effects which our results indicate are therefore accurate for the extremely dilute gas that we model. In real quantum gas experiments with higher α the same effects can be expected to be even larger than in our simulation.

4. Long-term evolution

We evolve in time by solving (2) numerically using the standard split-operator fast Fourier transform method [31] on a 32 768 $\times$ 512 grid, see figure 2. Due to the short time steps needed for stability of the split-operator method over long times, as well as the need for a very long grid in the x-direction in order to avoid finite-size effects even over this long time, the calculation is numerically demanding even with a good workstation: a single run of the simulation has required about seven days. We therefore report full results for only a single run. Other shorter-duration runs have shown that our one long run does appear to be qualitatively typical, and its long time and space scales provide ample numerical data for statistical analysis. Detailed quantitative results such as the power spectra we show below must nonetheless be considered tentative and preliminary, inasmuch as they represent a single run of the simulation and may well come out slightly differently in simulations from initial conditions that are different realizations of the truncated Wigner ensemble. More exhaustive investigation of the dependency on precise initial conditions must await future work.

In the beginning ($\tau = 0$) of our simulation the perturbations are too small to be seen. After some time ($\tau = 603$) instabilities seeded by the simulated quantum fluctuations have grown to form ripples between the horizons; these then deepen and break up into vortex pairs ($\tau = 630$). More and more vortices form ($\tau = 810$), until the ergoregion becomes a quasi-steady turbulent mess of vortices that continually form and escape (mostly through the white-hole horizon). A noisy pattern of sound waves is also continuously emitted by this turbulent ergoregion, through both horizons ($\tau = 1170$, enlarged version in figure 3). Because the excitations carry away energy from the supersonic region, the flow there gradually slows, while the condensate density in the ergoregion slowly rises to maintain continuity (see figure 4). Eventually the background velocity in the ergoregion falls below the local speed of sound, which rises with background density; the sonic horizons disappear, the subsonic superfluid flow is stable, and vortex production ceases ($\tau = 3960$).

Apart from the very early and late stages of our simulation there is no uniform value for the flow speed and the speed of sound, especially between the (initial) horizons, since the condensate density and phase are strongly varying in the turbulent region. However, we can define the averaged background flow speed $\bar{v}$ (by the phase gradient ignoring the phase perturbation due to the vortices) and averaged speed of sound $\bar{c}_2 = \sqrt{g\bar{\rho}}$ to see that the flow within $0 < x < L$ is *supersonic on average* until $\tau \sim 1000$, and thereafter subsonic on average (see figure 4). Examining figure 5 does not show any dramatic change in the character of the noisy sound waves that were emitted before and after $\tau \sim 1000$, however. This absence of qualitative change associated with subsonic average flow is not necessarily surprising, since even when the average flow is still supersonic within $0 < x < L$ the proliferation of vortices has already destroyed the irrotational character of the flow which the spacetime analogy assumes and it is no longer clear that speed of sound in laminar flow is even an important parameter for the turbulent region.

A (1+1)-dimensional scenario with atom sources and sinks, but otherwise similar to ours, has been studied in [20], building on [21]. Although this study did not model quantum fluctuations, it did incorporate random perturbations in the initial state and computed long-term evolution numerically. The open condensate system was found to evolve into a quasi-stationary phase of CESs from the initial ergoregion, analogous to our vortex production and emission. Similar behavior was also briefly reported in [10]. A significant difference in our two-dimensional scenario is that in the turbulent regions the coarse-grained net density of vortices can provide a curl of the long-wavelength velocity field [32], so that this flow is no longer irrotational. If regions of irrotational fluid flow are analogous to curved spacetime, a turbulent region is perhaps analogous to the stringy volume that lies inside the apparent horizon of a fuzzball [2].

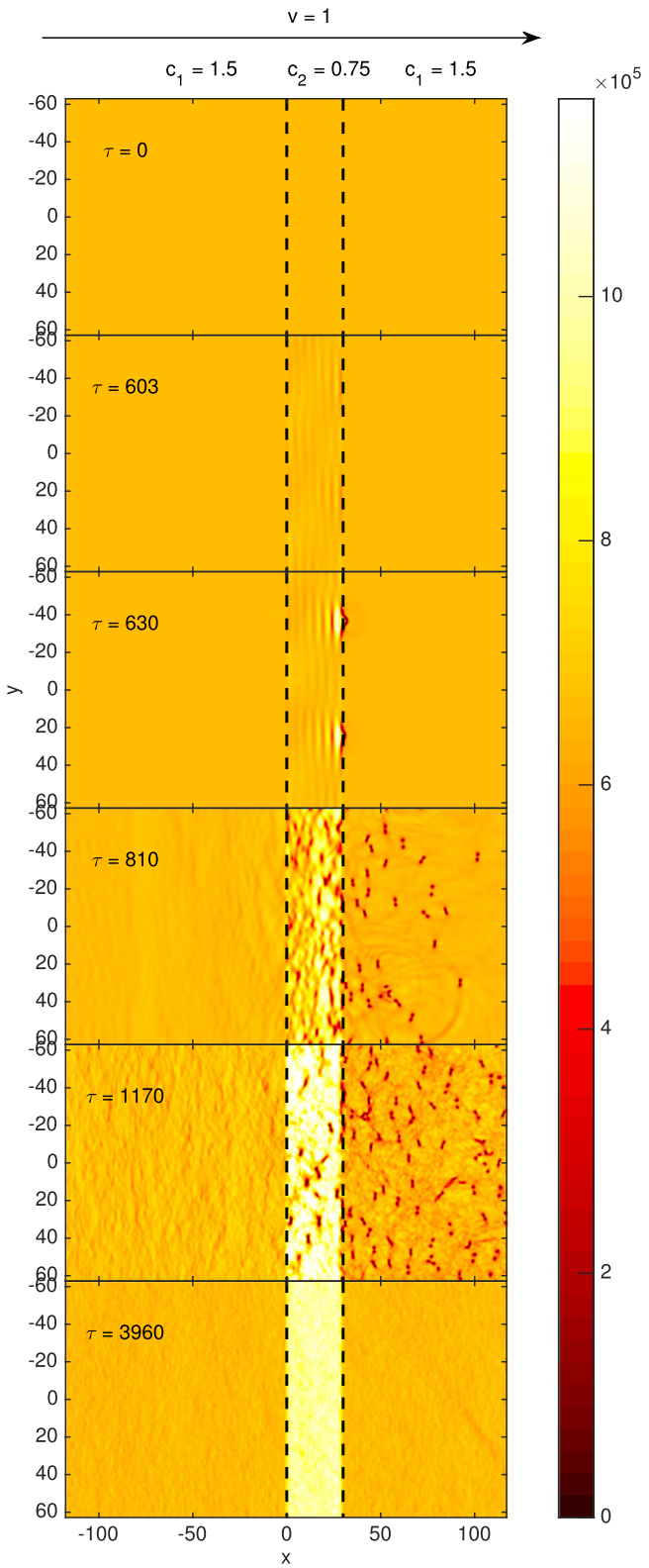

Figure 2. Temporal evolution of $|\Psi|^2$ for initial $c_1 = 1.5, c_2 = 0.75, L = 30$ and $\rho_0 = (200/d)^2 \doteq 6.6 \times 10^5$. The condensate flows in the positive x-direction with $v = 1$ initially. The dashed lines indicate the location of the horizons. Only a part of the x-range of the system is shown. There is no dissipation; the excitations visible at $\tau = 1170$ have simply propagated out of the field of view by $\tau = 3960$.

5. Quasi-steady radiation

Only a few close vortex–antivortex pairs emerge through the former black horizon, however, so the spacetime analogy remains valid there on longer wavelengths and the noisy pattern of sound waves visible in the left half of

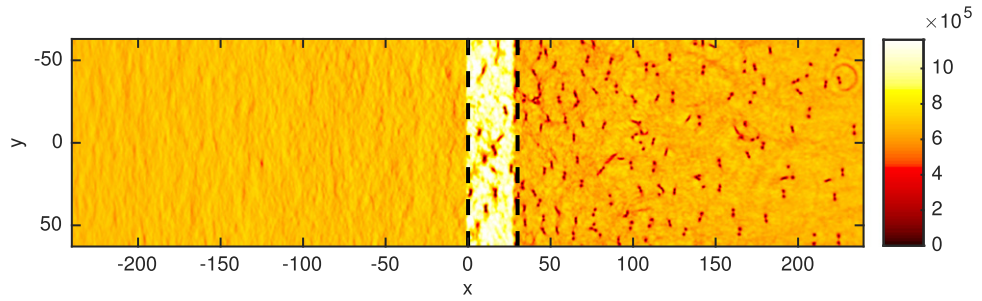

Figure 3. Same as figure 2 for $\tau = 1170$, enlarged to show detail.

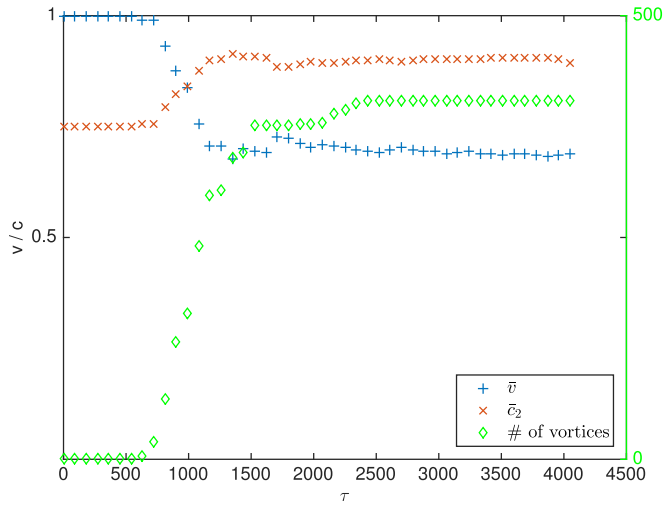

Figure 4. Average background flow velocity $\bar{v}$ (blue +), average speed of sound $\bar{c}_2$ (red crosses) and number of produced vortices (green diamonds, right y-axis). The flow is supersonic on average until $\tau \sim 1000$ and vortices are produced at a nearly constant rate from $\tau \sim 700$ until $\tau \sim 1600$.

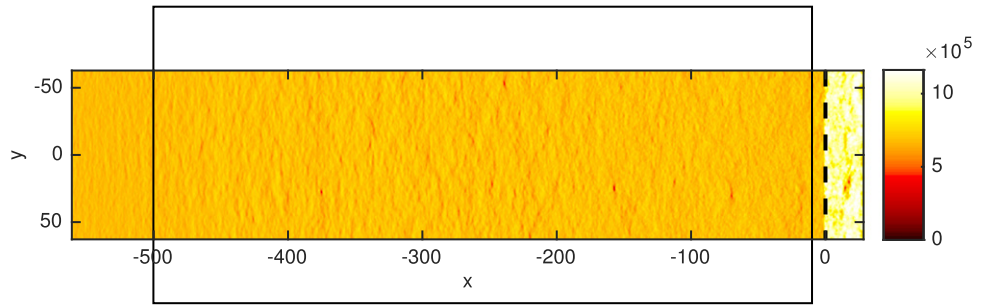

Figure 5. Quasi-steady radiation on the side of the former black hole at $\tau = 1530$. The box indicates the region that was used to calculate the power spectrum in figure 6.

figure 3 appears to be quasi-stationary. What is this emitted sound like, when it has grown from quantum fluctuations?

Our single typical $\Psi(x, y, \tau)$ appears to realize an ensemble within its evolution, in the sense that spacetime sub-volumes that are not too far apart from each other look like realizations of the same ensemble. To analyze the steady emission quantitatively, therefore, we choose a time ($\tau = 1530$) at which the emitted wave pattern appears homogeneously random within a large region, shown in figure 5. We then decompose $\delta\rho$ and $\delta\theta$ in Fourier modes, and count their energies, binned in k-space, as functions of BdG frequency. The results are shown in figure 6, with the analogous data from $\tau = 0$ for comparison. At $\tau = 0$ the energies follow the line $\langle E \rangle = \omega/2$ because the Wigner function from which they were randomly drawn provides this zero-point

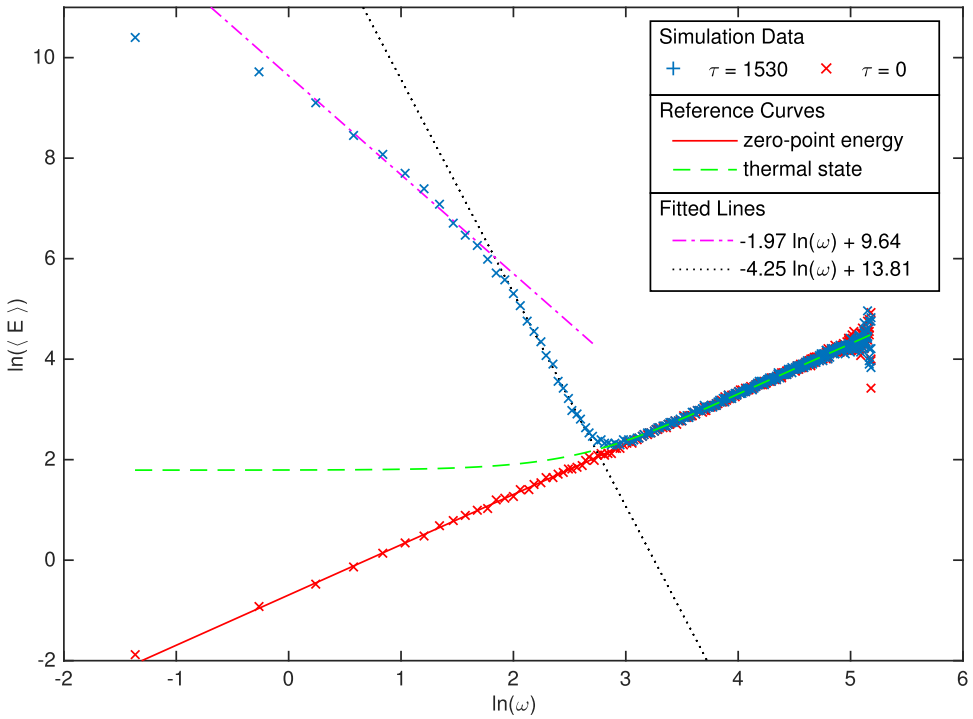

Figure 6. Energy spectrum of the excitations on the side of the former black hole at $\tau = 1530$ (blue +). The power spectrum is well described by power laws in three different ranges. The dashed green line shows the spectrum for a thermal state at $T \sim 6\ mv^2/k_B$ for comparison. The red crosses indicate the power spectrum at $\tau = 0$, which corresponds to the zero-point energy (solid red line).

energy. At high ω this vacuum noise remains essentially unchanged in the steady state epoch at $\tau = 1530$, but so much power has been generated at small ω that we need a log–log plot (figure 6) to see all of it. This high power low frequency radiation is clearly very different from thermal radiation (green line for $T \sim 6mv^2/k_B$, which is a fit to the high frequency tail of our data). The plot also seems to reveal two distinct power laws in addition to the zero-point energy at high frequencies. We find these power laws by fitting to our numerical data in the respective regions (fitted lines in figure 6). The points where the power laws turn over into each other fix two characteristic frequencies $\omega_1 \sim 6.2$ and $\omega_2 \sim 15.8$, which correspond to wavelengths on the order of (or somewhat shorter than) the healing length; we have no theoretical explanation for these frequencies. Sound emitted by turbulent regions is a subject in aeronautical engineering [33–35], and superfluid turbulence is an active topic in physics [36], but the sound emitted by a turbulent superfluid ergoregion does not yet seem to have a theory with which we can compare our numerical results for the power laws or characteristic frequencies. It also remains a question whether the observed turbulent state and radiation depend only on the mean-field parameters or are also sensitive to the initial distribution of fluctuations. Many more week-long runs, or some other form of analysis, will be needed in order to answer this question.

6. Discussion

The long-term evolution of a sonic black hole forces us to consider the meaning and value in general of experiments that are based on analogies. Theoretical mappings between very different physical systems are never exact; they are valid approximately, within certain regimes. Laboratory systems like ultracold gases can be tuned in so many ways that they can achieve many analogies, but even they cannot reproduce other systems exactly. Moreover, analogies usually only apply to some aspects of system behavior. The model system may reproduce some significant features of the target system while lacking others entirely.

The value of analog experiments does not only lie in offering oracle-like solutions to unsolved theoretical problems by exact analog computation, however. In cases like that of quantum gravity, so little is known about the target system that even limited analogies can be well worthwhile. The long-term evolution of black holes, for example, raises the very basic questions that have become known as the *black hole information paradox* [37]. A steadily radiating black hole will eventually have emitted energy comparable to its own rest energy, and so nonlinear back-reaction must eventually become important. If we abandon the linear approximation and consider the black hole and its radiation as a nonlinear dynamical system, however, the problem is not merely that we do not know exactly what theory of quantum gravity to apply. The severe problem is that it seems

impossible to reconcile the essential features of classical general relativistic black holes with *any* unitary quantum theory [37].

This means that it really is of fundamental interest to learn about any example of a nonlinear quantum theory which is known for certain to be self-consistent because it can be realized in the laboratory, and which includes states that can be mapped onto those of a quantum field in curved spacetime, but of which the evolution can be followed nonlinearly over long times. To simulate full quantum gravity in the laboratory is far too much to expect, but even a far less rigorous analogy can be a valuable contribution in a field where experimental data is rare.

In our case the nonlinear long-term evolution only preserves the analog spacetime outside the initial ergoregion. Inside, the flow becomes turbulent and the analogy breaks down. The instabilities to turbulent vortex production are not an unrelated phenomenon which masks steady thermal Hawking radiation, however. It is the same over-unity reflection due to mode-mixing at horizons which leads to stationary Hawking radiation for infinite ergoregions and to dynamical instabilities for finite ones. The specific way in which these instabilities saturate through vortex formation is a feature of nonlinear superfluid hydrodynamics rather than gravity, but the generic expectation of nonlinear quantum gravity is that it may also dramatically influence the interior structure of a black hole. The quasi-stationary epoch of our simulation indeed resembles the string-theoretic fuzzball scenario [2, 38], in which the smooth spacetime of classical general relativity likewise only survives outside the horizon.

The sonic radiation whose power spectrum is shown in figure 6 can be called Hawking radiation in the loose sense that it is emitted from the initial horizon region. It is clearly not thermal, however, at least not for a global temperature—the statistics of each mode in $\mathbf{k}$-space (not shown, [28]) do appear to be individually consistent with Boltzmannian ensembles ($\langle E^2\rangle / \langle E\rangle^2 \sim 2$), but with strongly $\mathbf{k}$-dependent temperatures. We have thus realized a scenario that was anticipated in [22] as a possible break down of the universality of thermal Hawking radiation, when it comes from a turbulent region inside the (former) black hole.

On the other hand we have also realized a scenario in which the curved-spacetime description remains valid outside the former black hole, which emits some kind of quasi-steady noisy radiation. The relaxation of our system into this non-thermally radiating state may be considered an example of pre-thermalization, inasmuch as the system approaches a quasi-stationary state which is not canonical equilibrium. Just as it is an important problem in the foundations of statistical mechanics to understand why some systems thermalize and others do not, so it is a good question to pose about quantum gravity, to ask which specific features of quantum gravitational dynamics may lead to thermally radiating black holes even beyond linearization, in contrast to systems like ours in which the generalized Hawking radiation is not thermal. Even when a physical analogy does not yield the right answer, it may supply the right question, and in this sense further study of sonic black holes, and the states into which they relax, will indeed be a valuable contribution to the difficult challenge of understanding true quantum black holes.

Acknowledgments

The authors acknowledge support from State Research Center OPTIMAS and the Deutsche Forschungsgemeinschaft (DFG) through SFB/TR185 (OSCAR).

Appendix. Sonic analogy

Here we show how the BdG equations in the hydrodynamic approximation can be mapped onto a massless scalar field equation in curved spacetime. This can be done in many ways, including some that clearly preserve the quantum nature of the BdG excitations. The shortest derivation proceeds, however, by implementing the hydrodynamic approximation already within the GPE ((2) in our main text) by defining $\Psi = \sqrt{\rho}\,\mathrm{e}^{\mathrm{i}\theta}$ for real ρ and θ, both arbitrary functions of space and time. One obtains

$$\partial_\tau \rho = -\boldsymbol{\nabla}\cdot(\rho\boldsymbol{\nabla}\theta), \tag{A.1}$$

$$\partial_\tau \theta = -\frac{1}{2}|\boldsymbol{\nabla}\theta|^2 - V - g\rho + \frac{1}{2\sqrt{\rho}}\nabla^2\sqrt{\rho} \tag{A.2}$$

$$\longrightarrow -\frac{1}{2}|\boldsymbol{\nabla}\theta|^2 - V - g\rho, \tag{A.3}$$

where the last line is the hydrodynamic approximation, valid whenever the condensate density varies slowly in space on the scale of the healing length $\xi = 1/\sqrt{g\rho}$. The long-wavelength limit of the BdG equations is then given by linearizing the hydrodynamic GP equations around an arbitrary background. Introducing the notation $\boldsymbol{v} = \boldsymbol{\nabla}\theta$ for the background velocity field, we find

$$\partial_\tau \delta\rho = -\nabla \cdot (\rho \nabla \delta\theta + v\delta\rho), \tag{A.4}$$

$$\partial_\tau \delta\theta = -v \cdot \nabla \delta\theta - g\delta\rho. \tag{A.5}$$

Introducing the component notation $\partial_\tau \to \partial_0$ and $\nabla \to \partial_i$ for Latin indices ranging between 1 and the number of spatial dimensions D, and applying the Einstein summation convention for the Latin indices, we can write these last equations as

$$\partial_i \rho\, \partial_i \delta\theta = -\partial_0 \delta\rho - \partial_i (v_i \delta\rho), \tag{A.6}$$

$$\delta\rho = -\frac{1}{g}(\partial_0 + v_i \partial_i)\delta\theta. \tag{A.7}$$

Defining the local (and in general, time-dependent) speed of sound $c(\boldsymbol{x}, \tau) \equiv \sqrt{g(\boldsymbol{x}, \tau)\rho(\boldsymbol{x}, \tau)}$, and introducing Einstein summation over Greek indices that run from 0 to D, these equations can be combined straightforwardly into the form

$$\partial_\mu K^{\mu\nu} \partial_\nu \delta\theta = 0 \tag{A.8}$$

for the following $(D+1) \times (D+1)$ matrix $K^{\mu\nu}$:

$$K^{00} = -\frac{\rho}{c^2}, \tag{A.9}$$

$$K^{i0} = K^{0i} = -\frac{\rho}{c^2} v_i, \tag{A.10}$$

$$K^{ij} = \rho\left(\delta_{ij} - \frac{v_i v_j}{c^2}\right). \tag{A.11}$$

We now compare (A.8) to the scalar wave equation for a massless field in a curved spacetime with metric tensor $g_{\mu\nu}$,

$$\frac{1}{\sqrt{-|g|}} \partial_\mu \sqrt{-|g|}\, g^{\mu\nu} \partial_\nu f = 0, \tag{A.12}$$

where $|g|$ denotes the determinant of $g_{\mu\nu}$ as a $(D+1) \times (D+1)$ matrix, and the contravariant metric tensor $g^{\mu\nu}$ is the inverse matrix g^{-1}. (We avoid the usual notation of plain g for the metric determinant, to avoid confusion with our condensate interaction strength.) It is clear that the linearized hydrodynamic equation would be of exactly the same form as the relativistic scalar wave equation, *if* we could find a metric tensor $g_{\mu\nu}$ such that the just-defined matrix $K^{\mu\nu}$ satisfies

$$K^{\mu\nu} = \sqrt{-|g|}\, g^{\mu\nu}. \tag{A.13}$$

For $D > 1$ this is easy: we merely need

$$g^{\mu\nu} = \frac{1}{\rho}\left(\frac{\rho}{c}\right)^{\frac{2}{1-D}} K^{\mu\nu}, \tag{A.14}$$

implying the covariant metric tensor

$$g_{00} = \left(\frac{\rho}{c}\right)^{\frac{2}{D-1}} (|v|^2 - c^2) \tag{A.15}$$

$$g_{i0} = g_{0i} = -\left(\frac{\rho}{c}\right)^{\frac{2}{D-1}} v_i \tag{A.16}$$

$$g_{ij} = \left(\frac{\rho}{c}\right)^{\frac{2}{D-1}} \delta_{ij}. \tag{A.17}$$

For the case $D = 3$ this agrees with the metric given in Unruh's original paper [3]; it is also a straightforward mapping for $D = 2$. For $D = 1$, however, it would be singular. This reflects the fact that the mapping does not work in $D = 1$.

The problem is that in $D = 1$ the determinant of $\sqrt{-|g|}\, g^{\mu\nu}$ is identically $-|g|\,|g^{-1}| \equiv -1$, for *any* metric $g_{\mu\nu}$. The determinant of the matrix $K^{\mu\nu}$ for $D = 1$, however, is $-\rho^2/c^2 = -\rho/g$. There is no way to make a non-flat metric in one-dimension without letting at least one of ρ and c vary with space or time, and although the interaction strength g can be controlled experimentally to some degree, the gas density is a dynamical variable that depends on initial conditions, and there is no way to simply lock g to follow the local value of ρ. One could try to give the background ρ and g the same spatial profile, but any mismatch would invalidate the Unruh analogy. The instabilities of one-dimensional sonic black holes to soliton formation would thus destroy the Unruh analogy, as ρ changed dynamically, even if $g \propto \rho$ could be achieved in the initial state.

One possible way of salvaging one-dimensional sonic horizons, apart from the interpretation as a $k_\perp = 0$ sector of a higher-dimensional model that we mentioned in our main text, would be to interpret the sound wave equation as the equation for a massless scalar field in a curved spacetime with a scalar dilaton field Φ as well as a metric, $\partial_\mu(\Phi\sqrt{-|g|}\,g^{\mu\nu}\partial_\nu f) = 0$. The dilaton field would have to have the particular configuration $\Phi \propto \rho/g$, fixed by the background condensate profile just as the metric is. This would then allow analog spacetime in one-dimensional condensates, but not analogs in which spacetime curvature is the only effect on field propagation, since the dilaton effects would also be important. It is also far from clear that the particular paired dilaton and metric configurations that are required by the Unruh analogy in one-dimension would be representative of black holes in general.

References

[1] Hawking S 1974 *Nature* **248** 30–1
[2] Mathur S 2005 *Fortschr. Phys.* **53** 793–827
[3] Unruh W 1981 *Phys. Rev. Lett.* **46** 1351–3
[4] Novello M, Visser M and Volovik G 2002 *Artificial Black Holes* (Singapore: World Scientific)
[5] Unruh W 1995 *Phys. Rev.* D **51** 2827–38
[6] Unruh W and Schützhold R (ed) 2007 *Quantum Analogues: From Phase Transitions to Black Holes and Cosmology* (Berlin: Springer)
[7] Weinfurtner S, Tedford E W, Penrice M C, Unruh W G and Lawrence G A 2011 *Phys. Rev. Lett.* **106** 021302
[8] Rousseaux G, Mathis C, Maissa P, Philbin T G and Leonhardt U 2008 *New J. Phys.* **10** 053015
[9] Corley S and Jacobson T 1999 *Phys. Rev.* D **59** 124011
[10] Garay L, Anglin J, Cirac J and Zoller P 2001 *Phys. Rev.* A **63** 023611
[11] Garay L, Anglin J, Cirac J and Zoller P 2000 *Phys. Rev. Lett.* **85** 4643–7
[12] Finazzi S and Parentani R 2010 *New J. Phys.* **12** 095015
[13] Busch X and Parentani R 2014 *Phys. Rev.* D **89** 105024
[14] de Nova J R M, Sols F and Zapata I 2015 *New J. Phys.* **17** 105003
[15] Boiron D, Fabbri A, Larré P E, Pavloff N, Westbrook C I and Ziń P 2015 *Phys. Rev. Lett.* **115** 025301
[16] Finazzi S and Carusotto I 2014 *Phys. Rev.* A **90** 033607
[17] Lahav O, Itah A, Blumkin A, Gordon C, Rinott S, Zayats A and Steinhauer J 2010 *Phys. Rev. Lett.* **105** 240401
[18] Steinhauer J 2014 *Nat. Phys* **10** 864
[19] Steinhauer J 2016 *Nat. Phys* **12** 959
[20] de Nova J, Finazzi S and Carusotto I 2016 *Phys. Rev.* A **94** 043616
[21] Michel F and Parentani R 2015 *Phys. Rev.* A **91** 053603
[22] Unruh W G and Schützhold R 2005 *Phys. Rev.* D **71** 024028
[23] Sinatra A, Lobo C and Castin Y 2002 *J. Phys. B: At. Mol. Opt. Phys.* **35** 3599
[24] Ruostekoski J and Martin A 2013 *The Truncated Wigner Method for Bose Gases* (London: Imperial College Press) pp 203–14
[25] Blakie P, Bradley A, Davis M, Ballagh R and Gardiner C 2008 *Adv. Phys.* **57** 363
[26] Pitaevskii L and Stringari S 2003 *Bose–Einstein Condensation* (*International Series of Monographs on Physics*) (Oxford: Clarendon)
[27] Stabel P and Anglin J in preparation
[28] Bürkle R, Gaidoukov A and Anglin J in preparation
[29] Zapata I, Albert M, Parentani R and Sols F 2011 *New J. Phys.* **13** 063048
[30] Lee T, Huang K and Yang C 1957 *Phys. Rev.* **106** 1135–45
[31] Weideman J and Herbst B 1986 *SIAM J. Numer. Anal.* **23** 485–507
[32] Feynman R 1955 *Prog. Low Temp. Phys.* **1** 17–53
[33] Lighthill M 1952 *Proc. R. Soc.* A **211** 564–87
[34] Lighthill M 1954 *Proc. R. Soc.* A **222** 1–32
[35] Dowling A and Hynes T 2004 *Eur. J. Mech.* B **23** 491–500
[36] Tsatsos M C, Tavares P E, Cidrim A, Fritsch A R, Caracanhas M A, dos Santos F E A, Barenghi C F and Bagnato V S 2016 *Phys. Rep.* **622** 1–52
[37] Mathur S 2009 *Class. Quantum Grav.* **26** 224001
[38] Chen F, Michel B, Polchinski J and Puhm A 2015 *J. High Energy Phys.* JHEP02(2015)081